19th Australasian Fluid Mechanics Conference
Melbourne, Australia
8-11 December 2014

A Study of Piezoelectric Energy Harvesters in Smooth and Turbulent Flows: How Might They Perform in Real-World Conditions?

J. M. McCarthy[1], A. Deivasigamani[1], S. Watkins[1], S. J. John[1] and F. Coman[2]

[1]School of Aerospace, Mechanical and Manufacturing Engineering
RMIT University, Bundoora, Victoria 3081, Australia

[2]Fabrics & Composites Science & Technology Pty. Ltd.
South Carlton, Victoria 3053, Australia

Abstract

In this work, a single "leaf-stalk"-type piezoelectric energy harvester was studied in smooth flow and aspects of replicated ABL turbulence (12.7% intensity, 310-mm longitudinal integral length scale). The harvester was yawed and pitched with respect to the prevailing wind direction, so that the performance of the harvester in terms of mean output power could be observed. Key findings of the study were: 1) off-axis flow conditions rapidly degraded the mean output power of the harvester; 2) turbulence acted similarly to a dynamic damping mechanism; 3) for parallel flow, turbulence diminished the power outputs relative to smooth flow and for off-axis flow, the turbulence enhanced the power outputs relative to smooth flow.

Introduction

Extracting energy from wind has been the focus of research and development for centuries. The vast majority of developments have been in smooth flows (either experimental or computational) with recent work including replicating the effects of the Atmospheric Boundary Layer (ABL), where it has been shown that turbulence increases structural loading and decreases power output [6]. However, there are new wind-energy technologies emerging that show potential for low, local power generation systems (e.g. figure 1). Such Ultra-low power (ULP) technologies could be a source of power for low-energy technologies such as wireless sensor nodes or LED lighting in urban-based buildings; the technology could also be considered safer, quieter and more aesthetically pleasing than small-scale, urban-based wind turbines [10]. These technologies involve piezoelectric films fluttering in a fluid stream, and can be grouped into two types; harvesters that self-excite in flutter, and those where flutter is induced by a vortex-shedding upstream bluff body, known as Vortex-Induced Vibrations (VIV). Extensive treatments of self-exciting flutter have been realised elsewhere [e.g. 3, 9, 13, 14], but here we restrict ourselves to exploiting VIV to generate power.

Energy harvester utilising VIV-type flutter involves analysis of the structural and fluid-forcing response spectrums so that the shedding frequency may be tuned to the resonant frequencies of the structure, resulting in greater deformations and power outputs. Research into VIV-type harvesting had been conducted in [2]; their work consisted of a thin membrane containing piezoelectric patches, immersed in the flow downstream of a circular cylinder shedding vortices that impinged on the membrane, periodically deforming it and generating power. In an energy harvesting context, VIV-type flutter is potentially more beneficial since the vortex shedding frequency may be tuned to the structure's natural frequency. It was found that by using this method of tuning for parallel flow conditions, power outputs increased significantly due to large-amplitude vibrations. The harvesters need to be rigidly held in the fluid stream, and the root of the piezoelectric stalk must be clamped so that bending strains are developed, which convert to power output. This negates the possibility of incorporating individual-harvester self-alignment mechanisms at the root of the stalk, which would permit the harvester to align with the mean wind direction. In the case of VIV-type harvesters, the clamping-base cross-sectional shape is a key parameter, though in the case of the suggestion made in [8] a circular cross-section was envisioned so as to mimic a tree-like appearance. The variation in positioning of the harvester, coupled with the variability of wind direction means that an individual harvester may experience a wide range of wind conditions. Interestingly, there has been little or no work done on examining the effect of off-axis and turbulent flow conditions on the output power from these harvester types. Thus, here we examine the cases where the wind is off-axis, and the harvester is immersed in aspects of replicated ABL turbulence.

Figure 1. The artificial "tree" concept, utilising piezoelectric materials to harvest ambient flow energy, as proposed initially in [8].

Methods and Instrumentation

Two wind tunnels were used for this study, one for smooth flow and the second for turbulent flow.

Aeronautical Wind Tunnel

The smooth-flow work was conducted in the RMIT University Aeronautical Wind Tunnel (AWT). This tunnel is a closed-circuit design consisting of a 100-kW DC motor driving a six bladed fan. The test section is octagonally shaped and is 2,100-mm long, 1,070-mm high and 1,320-mm wide. Upstream of the test section there is a 4:1 contraction ratio and anti-turbulence screens conditioning the flow, such that across a wide range of wind speeds the average longitudinal turbulence intensity component is less than 0.3% [7]. Flow speed measurements were made via a Baratron® pressure-based system and a pitot-static tube inserted at the entrance to the test section. Tunnel blockage was insignificant.

Industrial Wind Tunnel

The RMIT University Industrial Wind Tunnel (IWT) was used for the work in turbulent flow. The tunnel is a closed-circuit design with a 200-kW thyristor controlled DC motor driving a six bladed fan. The test section is rectangularly shaped and is 9-m long, 2,000-mm high and 3,000-mm wide. A 2:1 contraction is present before the test section, and the anechoic turning vanes reduce the acoustic signature of the fan. The inlet of the test section could accommodate installation of turbulence grids of varying sizes, so that turbulence of different intensities and scales could be generated. A Baratron® system was also used for monitoring flow speeds in a similar manner to the AWT. Integral length scales similar to the harvester size, and relatively high turbulence intensities were desired. This is because length scales similar to the immersed structure size will affect the dynamics of the structure more than much larger or much smaller scales [21]. Also, the relatively high longitudinal turbulence intensity is more indicative of ABL turbulence. A planar grid, previously designed in [12], was installed at the inlet of the test section, see figure 2. This grid consisted of 300-mm wide chipboard with 600-mm spacings between the boards, which produced a decaying turbulence intensity along the length of the test section. Relatively high levels of turbulence intensity are possible with this grid type, but there was a trade-off between achieving a high turbulence intensity of relatively large scale, and achieving well-mixed turbulence. The region near the grids consisted of discrete jets and wakes, which rendered a non-flat velocity profile. The downstream distance of 7.75 m as utilised previously in [11] and [19] was chosen, as the turbulence was well mixed, with a nominally flat velocity profile and a longitudinal turbulence intensity of around 12.7%. Longitudinal integral length scales were also documented in [19] as 310 mm at this downstream location, roughly twice the physical length of the harvester. The tunnel was then calibrated and the local wind speed was then varied.

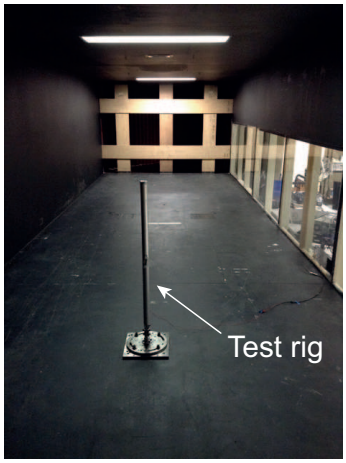

Figure 2. The setup in the IWT. The test rig may be seen and also the turbulence-generation grids at the inlet of the test section.

Harvester and Test Rig Data

The harvesters used here were congruent to those studied in [14, 16, 17]. The testing rig consisted of a 41-mm diameter, 800-mm long aluminium capped cylinder fitted to a base that could rotate both about the cylinder's longitudinal (yaw) and radial (pitch) axes. The rig was designed for EIE-type flutter in smooth flow. The diameter-based Reynolds number range for the flow past the cylinder was $\approx 8 \times 10^3$ to 2.2×10^4. Sizing the cylinder diameter to the harvester fundamental bending frequency of 4.1 Hz was impractical, as the cylinder base would have become cumbersome and induced tunnel blockage. Instead, the cylinder was sized such that the vortex shedding frequency as calculated from a cylinder-normal Strouhal number of 0.2 matched the harvester's second natural frequency of 15 Hz at 3 ms^{-1}. A schematic defining sign convention for the yaw and pitch angles is given in figure 3.

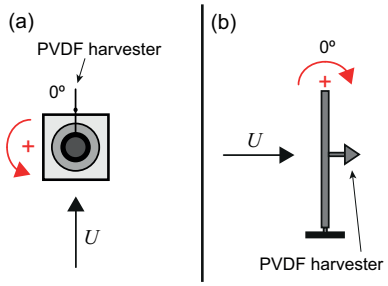

Figure 3. Sign convention for (a) yaw angle and (b) pitch angle. U is the free-stream flow speed.

The mean power output of the harvester was calculated as

$$P_{mean} = \frac{V_{RMS}^2}{R_L} \tag{1}$$

where V_{RMS} is the root-mean-square voltage output and R_L is the load resistance. The output power was normalised by the PVDF patch area, to permit comparison with existing renewable-energy technologies such as Photo-Voltaics (PVs) or wind turbines. The normalised power P_{norm} was plotted against the [yaw, pitch] angle and the wind speed U on three-dimensional scatter plots, with error bars at 95% confidence plotted on some of the angles to verify repeatability.

Results and Discussion

The yaw and pitch-angle results in smooth flow are presented in figures 4 and 5 respectively, while the results in turbulent flow are given in figures 6 and 7. Due to the bi-stable nature of the harvester at 180°, error was quite prevalent; however, the observed flutter behaviour was consistent across tests for the 3 and 4 m/s cases. The dynamic pressure of the flow forced the PVDF to bend back against itself but the strain energy developed in the PVDF was greater than the flow kinetic energy, and the PVDF would bend back to its original position; asymmetric, sporadic flutter resulted, generating some power. This bi-stable behaviour ceased at wind speeds greater than 4 m/s, when the flow kinetic energy was sufficient to prevent the harvester from returning to its undeflected position. This peculiar behaviour was actually more pronounced in turbulence than in smooth flow, due to the greater local flow fluctuations.

In work elsewhere [15], it was discovered that for this particular harvester configuration and for 3 – 8 m/s, the power output increased approximately as $\sqrt{U}$ for parallel flow; this is observed here in the 0° data, and to some extent, the 45° data. The power output decreased significantly as the angle deviated from 0° in every instance of angle and flow condition. Increasing the yaw angle meant that vortex shedding from the EIE rig in the harvester plane was suppressed, and gradual transition away from Limit-Cycle Oscillations (LCOs) resulted in lower power output, see [1]. It is seen in figure 4 that for $\geq 90°$, negligible power is generated for every wind speed tested, except for the two anomalies at 180°. LCOs were still observed at a yaw angle of 45°, but the harvester tip amplitudes were lessened considerably. At higher yaw angles, the dynamic pressure prevented harvester LCOs. Low-frequency oscillations were observed, but were stochastic in nature. Similar to yaw angle, significant decreases in output occurred for pitch angles greater or lesser than

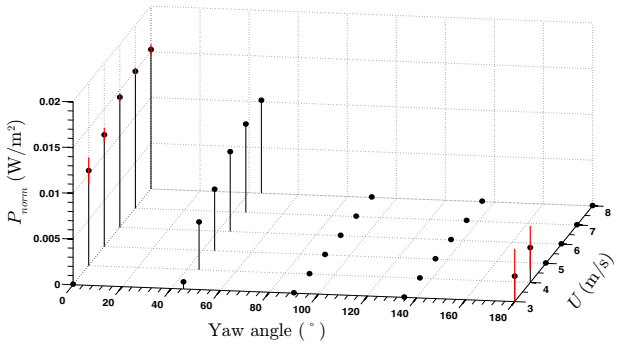

Figure 4. P_{norm} of the harvester versus yaw angle and wind speed in smooth flow, with zero applied pitch angle. Error is denoted by vertical red bars on the 0 and 180° cases.

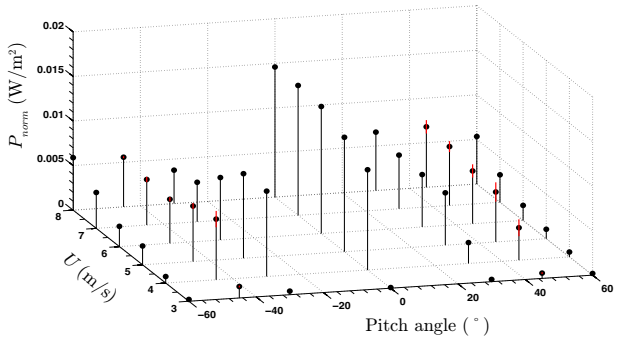

Figure 5. P_{norm} of the harvester versus pitch angle and wind speed in smooth flow, with zero applied yaw angle. Error is denoted by vertical red bars on the ±45° cases.

0°. The chief disparity between the yaw- and pitch-angle cases was that the harvester remained within the cylinder wake, regardless of pitch angle. The vortex shedding mechanisms also differed for non-zero pitch angles. At pitch angles of ±30° and subcritical Reynolds numbers, [20] observed that the wake vortices convected approximately in the direction of $U\cos\alpha$, where α is the pitch angle. At pitch angles of ±60°, the direction of the vortices varied in two noticeable directions along the cylinder span, with vortices sufficiently far from the cylinder free end propagating in the direction of $U\cos\alpha$, and vortices near the free-end region travelling at angles greater than $\cos\alpha$. It is likely that the harvester was in the region where the vortices travelled in the direction of $U\cos\alpha$. A normalised Strouhal number was defined in [18] as $\mathrm{St}/\mathrm{St}_N$, where St is the measured value of Strouhal number, and St_N is $f_s d/U$, f_s is the vortex shedding frequency. At 0° pitch, $\mathrm{St}/\mathrm{St}_N = 1$ and the *Independence Principle* is valid; at ±60° pitch, $\mathrm{St}/\mathrm{St}_N$ reduced to roughly 0.6 (A 40% disparity from the Independence Principle prediction), implying that the shedding frequency has decreased. This may be attributed to a decrease in vortex strength with increasing pitch angle [22]. This is a likely cause for the decreased power output from the harvester at non-zero pitch angles, as the harvester is not sensitive to solely the normal flow component in the EIE-rig near wake, but is subject to the three-dimensional wake effects prevalent at non-zero pitch.

The spectral density of the voltage signal reveals the nature of how turbulence affects the harvester performance. In figure 8, the spectral density estimate is given for wind speeds of 4 and 5 m/s in smooth and turbulent flow at 0° yaw and pitch angle. The peak is the dominant flutter frequency of the harvester, which changes with wind speed. In smooth flow (figure 8a), the peak is

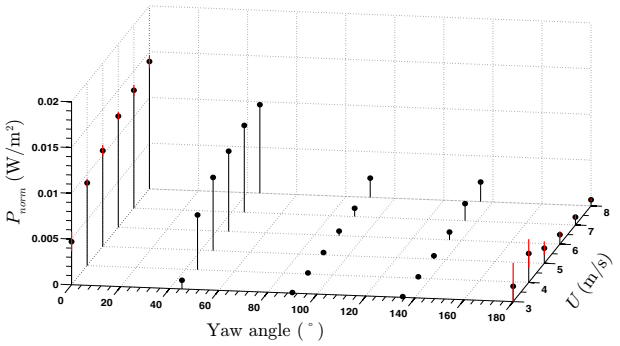

Figure 6. P_{norm} of the harvester versus yaw angle and wind speed in turbulent flow, with zero applied pitch angle. Error is denoted by vertical red bars on the 0 and 180° cases.

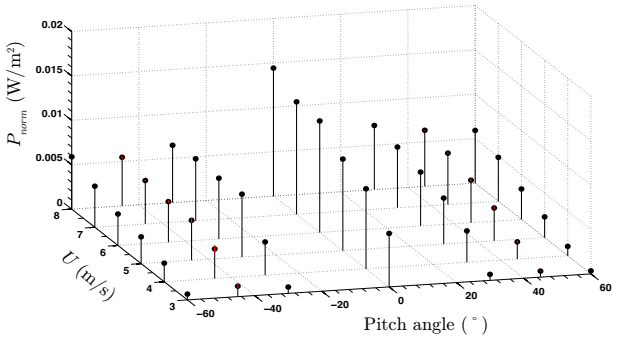

Figure 7. P_{norm} of the harvester versus pitch angle and wind speed in turbulent flow, with zero applied yaw angle. Error is denoted by vertical red bars on the ±45° cases.

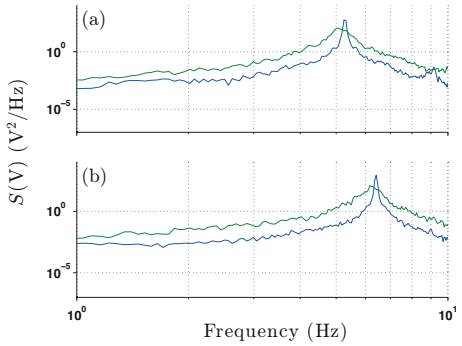

Figure 8. Voltage spectral density from the harvester at (a) 4 m/s, in (—) smooth and (—) turbulent flow; (b) 5 m/s in smooth and turbulent flow. The yaw and pitch angle is 0°.

more discrete because the harvester is fluttering in LCOs. However, in turbulence it is evident that there is a more broadband response. This agrees with findings in [4] and [5] for similar turbulence intensities, integral length-scales and Reynolds numbers. This type of behaviour appears akin to decreasing the quality factor, Q, of a discrete resonant peak, where;

$$Q = \frac{1}{2\zeta}. \tag{2}$$

Here, ζ is the viscous damping ratio of a system. This suggests that turbulence in the flow dampens the harvester flutter response and if figures 4 and 6 are compared, it can be seen that at 0°, the output power in turbulence is less than in smooth

flow. Interestingly, the power output in turbulence at higher angles and wind speeds was greater, suggesting that the higher frequency energy of fluctuations in the inertial subrange are transduced to power output through the harvester, whereas in smooth flow these fluctuations are significantly lower.

Conclusions

A piezoelectric energy harvester was examined in smooth and aspects of replicated ABL turbulence at differing wind velocities. The results of the study are as follows:

- The harvester performance degrades significantly as the angle to the wind is increased.
- The harvester performance is degraded in turbulence compared to smooth flow for parallel flow.
- The harvester performance is enhanced in turbulence compared to smooth flow for off-axis flow at higher wind speeds.

Further studies would involve optimising a harvester to operate in turbulent-flow conditions.

Acknowledgements

This work was funded under Australian Research Council (ARC) Linkage grant LP100200034 in conjunction with the Partner Organisation – Fabrics & Composites Science & Technology (FCST) Pty Ltd.

*

References

[1] Alben, S. and Shelley, M. J., Flapping states of a flag in an inviscid fluid: Bistability and the transition to chaos, *Physical Review Letters*, **100**, 2008, 074301–1 – 4.

[2] Allen, J. J. and Smits, A. J., Energy harvesting eel, *Journal of Fluids and Structures*, **15**, 2001, 629–640.

[3] Argentina, M. and Mahadevan, L., Fluid-flow-induced flutter of a flag, *Proceedings of the National Academy of Sciences of the United States of America*, **102**, 2005, 1829–34.

[4] Basu, R., Aerodynamic forces on structures of circular cross-section. part 2. the influence of turbulence and three-dimensional effects, *Journal of Wind Engineering and Industrial Aerodynamics*, **24**, 1986, 33 – 59.

[5] Blackburn, H. and Melbourne, W., Lift on an oscillating cylinder in smooth and turbulent flow, *Journal of Wind Engineering and Industrial Aerodynamics*, **41**, 1992, 79 – 90.

[6] Burton, T., Sharpe, D., Jenkins, N. and Bossanyi, E., *Wind Energy Handbook*, John Wiley & Sons, 2001.

[7] Creazzo, J., *The interaction between a non-imbedded longitudinal vortex and turbulent boundary layer under the influence of a stream-wise pressure gradient*, PhD thesis, School of Aerospace, Mechanical and Manufacturing Engineering, RMIT University, Melbourne, Australia, 1999.

[8] Dickson, R., *New Concepts in Renewable Energy*, Lulu Enterprises, Inc., 2008.

[9] Eloy, C., Souilliez, C. and Schouveiler, L., Flutter of a rectangular plate, *Journal of Fluids and Structures*, **23**, 2007, 904–19.

[10] Encraft, Final report (Warwick Microwind Trial project), Technical report, 2009.

[11] Fisher, A., *The effect of freestream turbulence on fixed and flapping micro air vehicle wings*, PhD thesis, RMIT University, 2013.

[12] Grusovin, M. P., *Modeling of Atmospheric Boundary Layer in the RMIT Industrial Wind Tunnel*, Undergraduate thesis, RMIT University School of Aerospace, Mechanical and Manufacturing Engineering, 2006.

[13] Huang, L., Flutter of cantilevered plates in axial flow, *Journal of Fluids and Structures*, **9**, 1995, 127–147.

[14] Li, S. and Lipson, H., Vertical-stalk flapping-leaf generator for wind energy harvesting, in *ASME Conference on Smart Materials, Adaptive Structures and Intelligent Systems, SMASIS2009, September 21 - September 23*, American Society of Mechanical Engineers, Oxnard, CA, United states, 2009, volume 2.

[15] McCarthy, J., Deivasigamani, A., John, S., Watkins, S. and Coman, F., The effect of the configuration of the amplification device on the power output of a piezoelectric strip, in *ASME Conference on Smart Materials, Adaptive Structures and Intelligent Systems, SMASIS2012, Sept. 19 - 21*, American Society of Mechanical Engineers, Stone Mountain, Georgia, USA, 2012, number 7951.

[16] McCarthy, J., Deivasigamani, A., Watkins, S., John, S., Coman, F. and Petersen, P., Downstream flow structures of a fluttering piezoelectric energy harvester, *Experimental Thermal and Fluid Science*, **51**, 2013, 279–290.

[17] McCarthy, J., Deivasigamani, A., Watkins, S., John, S., Coman, F. and Petersen, P., On the visualisation of flow structures downstream of fluttering piezoelectric energy harvesters in a tandem configuration, *Experimental Thermal and Fluid Science*, **57**, 2014, 407–419.

[18] Ramberg, S. E., The effects of yaw and finite length upon the vortex wakes of stationary and vibrating circular cylinders, *Journal of Fluid Mechanics*, **128**, 1983, 81–107.

[19] Ravi, S., *The Influence of Turbulence on a Flat Plate Airfoil at Reynolds Numbers Relevant to MAV's*, PhD thesis, RMIT University School of Aerospace, Mechanical and Manufacturing Engineering, 2011.

[20] Thakur, A., Liu, X. and Marshall, J., Wake flow of single and multiple yawed cylinders, *ASME Journal of Fluids Engineering*, **126**, 2004, 861–870.

[21] Watkins, S., Loxton, B. J., Milbank, J. and Melbourne, W. H., Replication of atmospheric conditions for the purpose of testing MAV's: MAV flight environment project final report, Technical report, RMIT University, Melbourne, Australia, 2005.

[22] Zhou, T., Razali, S. F. M., Zhou, Y., Chua, L. P. and Cheng, L., Dependence of the wake on inclination of a stationary cylinder, *Experiments in Fluids*, **46**, 2009, 1125–1138.